ISSN 2079-1704. Хімія, фізика та технологія поверхні. 2023. Т. 14. № 2. С. 173-181

PACS numbers: 61.48; 61.82Pv; 61.82Rx; 62.23Pq; 73.63 doi: 10.15407/hftp14.02.173

S.M. Makhno [1, 2, 3], O.M. Lisova [3], G.M. Gunya [3], P.P. Gorbyk [3], M.T. Kartel [1, 2, 3]

SYNTHESIS AND ELECTROPHYSICAL PROPERTIES OF NANOSTRUCTURED COMPOSITES NiCo/$BaTiO_3$ AND NiCo/TiO_2

[1] Ningbo University of Technology
201 Fenghua Road, Ningbo, 315211, China
[2] Ningbo Sino-Ukrainian New Materials Industrial Technologies Institute
Kechuang building, N777 Zhongguan road, Ningbo, 315211, China
[3] Chuiko Institute of Surface Chemistry of National Academy of Sciences of Ukraine
17 General Naumov Str., Kyiv, 03164, Ukraine, E-mail: oksana.garkusha@gmail.com

Nanocomposites containing components with semiconductor, ferroelectric, and ferromagnetic properties have attracted considerable attention of specialists due to the range of possible applications, including catalysis and electrocatalysis, electrode materials for solar and fuel cells, capacitors, electrical and biosensors, anti-corrosion coatings and much more. In recent years, both fundamental and applied interest in this direction of research is due to the possibility of creating a new type of controlled microwave devices and tools.

The aim of the work is to develop methods for the synthesis of nanostructured NiCo composites based on $BaTiO_3$ and TiO_2, as well as to find the differences and regularities of their physicochemical properties. Two series of samples with different content of NiCo nanoparticles based on titanium oxide (TiO_2) and barium titanate ($BaTiO_3$) were obtained. NiCo particles were obtained by the method of chemical precipitation of nickel and cobalt carbonates in equal parts from a hydrazine hydrate solution at the temperature of 350 K.

The results of X-ray phase analysis indicate the chemical purity of the obtained samples. The values of ε', ε'' at a frequency of 9 GHz for the NiCo/$BaTiO_3$ system are twice as high compared to NiCo/TiO_2 for the corresponding values of the NiCo content, which is due to the higher values of ε', ε'' of the initial barium titanate. Electrical conductivity of NiCo/$BaTiO_3$ system changes by six orders of magnitude, which indicates the formation of a continuous percolation cluster of metal particles on the surface of dielectric $BaTiO_3$ particles. The composites are heat-resistant up to 630K, as shown by the method of thermogravimetry and pronounced magnetic properties.

The program for calculating frequency dependences of reflection and absorption coefficients in a complex form has been developed. EMF absorption for composites from the radiation frequency and the position of the minima of these characteristics, which agree satisfactorily with the experiment. The obtained composites can be promising components for obtaining composite systems and paints for protection against electromagnetic radiation.

***Keywords**: nanocomposites, nanoparticles, ferromagnetic, electromagnetic wave, electrical conductivity*

INTRODUCTION

Nanocomposites containing components with semiconductor, ferroelectric, and ferromagnetic properties have attracted considerable attention of specialists for a long time due to the range of possible applications [1–4]. Catalysis and electrocatalysis [2, 5, 6] are promising fields of implementation of similar structures. In electronics, such composites are used as electrode materials for solar and fuel cells, capacitors [4] electrical and biosensors [7–9], as well as anti-corrosion coatings and much more. They acquire better catalytic, thermal, optical, electrical, and magnetic properties compared to monometallic and bimetallic particles without the presence of a matrix, which not only plays the role of a substrate, but is a functionally active element [10, 11]. Composites using a barium titanate or titanium dioxide substrate and obtained by various methods by doping with magnetic and non-magnetic nanoparticles are widely studied [12–15].

In recent years, both fundamental and applied interest in this direction of research is due to the possibility of creating a new type of controlled microwave devices and tools. The synergetic effect of polarization and conductivity is extremely important. Therefore, to improve the characteristics of microwave absorption, the structure of the absorbing element must satisfy several requirements simultaneously. It has a sufficiently high level of inhomogeneity, i.e., a significant interface between individual components, which creates regions with a high

degree of polarization, and is also in the state of a branched percolation cluster to ensure conduction losses [16–18].

The absorbing ability of composites depends on the level of dielectric and magnetic losses and their ratio, on the size of the particles and periodic elements they form, the thickness of the interfacial layers and their structure [19–21]. Absorbent materials, in addition to economic efficiency, should have wide absorption bands, be light and thin. Core-shell structures, hollow microspheres are attractive for facile broadband microwave absorption due to their multiphase the presence of voids. At present, a significant number of various hybrids consisting of carbon material and magnetic nanoparticles have been developed, in which the synergistic effect of several loss mechanisms simultaneously operates. Impedance matching and excellent attenuation characteristics can be optimized in such composites. For example, it was reported in [15] that flower-shaped Ni/C microspheres are characterized by strong electromagnetic wave scattering.

The possibility of creating microwave devices with double control by magnetic or electrical methods [22–24] based on layered structures of the ferromagnet/ferroelectric type has increased with the development of technologies for the production of ceramic ferroelectrics (barium titanate ($BaTiO_3$), strontium titanate ($SrTiO_3$)) with a wide range of dielectric change permeability

The aim of the work is to develop methods for the synthesis of nanostructured NiCo composites based on $BaTiO_3$ and TiO_2, as well as to find the differences and regularities of their physicochemical properties.

RESEARCH METHODOLOGY AND MATERIALS

Two series of samples with different content of NiCo nanoparticles based on titanium oxide (TiO_2) and barium titanate ($BaTiO_3$) were obtained. NiCo particles were obtained by the method of chemical precipitation of nickel and cobalt carbonates in equal parts from a hydrazine hydrate solution at the temperature of 350 K. Ready powders TiO_2 (rutile structure, R-960 produced by DuPont) and $BaTiO_3$ (CAS 12047-27-7, produced “Sigma-Aldrich”, particle size 2 μm). For the synthesis of NiCo/TiO_2 and NiCo/$BaTiO_3$ composites, the methodology was modified: with constant stirring of TiO_2 (or $BaTiO_3$) aqueous suspensions, co-precipitation of a solution of nickel and cobalt carbonates with the same content at the boiling temperature of hydrazine hydrate was carried out. The product was washed with distillate to neutral pH, filtered, dried at a temperature of 353 K.

The X-ray phase analysis of the composites was carried out by the powder diffractometry method on a DRON-4-07 diffractometer in the CuK_α radiation of the anode line with a nickel filter in the reflected beam with the Brague–Bretano shooting geometry.

The study of the real (ε′) and imaginary (ε″) components of the complex dielectric constant of composites was carried out in the ultrahigh-frequency (HF) range of 8–12 GHz using an interferometer based on an RFK2-18 phase difference meter and a P2-60 electrodeless standing wave and attenuation coefficient meter method. The electrical conductivity at low frequencies 0.1; 1 and 10 kHz by the two-contact method using an E7-14 immittance meter [25]. The relative error of determining ε′, ε″, μ′, μ″, σ, did not exceed ~5 %.

The thermal destruction of the composites was investigated by the method of thermogravimetry with the help of a “Q-1500 D” derivatograph. Samples weighing 100 ± 5 mg were heated in ceramic crucibles at a rate of 10 degrees/min in an air atmosphere.

Determination of the specific surface area of the samples was carried out by the method of thermal desorption of argon (GOST 23401 - 90) at 393 K.

RESULTS AND THEIR DISCUSSION

The results of X-ray phase analysis (Fig. 1) indicate the presence of titanium dioxide, nickel, cobalt, and the absence of reflexes of incoming carbonates. The peaks 52.2° (111) and 60.9° (200) of JCPDS #89-7128 may correspond to nickel particles.

The crystal lattice of cobalt received peaks at 52.2° (111), 56.6° (100), 61.2° (200), JCPDS #89-7373. The sizes of crystals treated according to the Scherrer equation for Ni and Co nanoparticles are 18 nm, 0.13NiCo/0.87$BaTiO_3$ – 20 nm, 0.7NiCo/0.3$BaTiO_3$ – 28 nm, 0.13NiCo/0.87TiO_2 – 28 nm, 0.7NiCo/0.3TiO_2 – 32 nm.

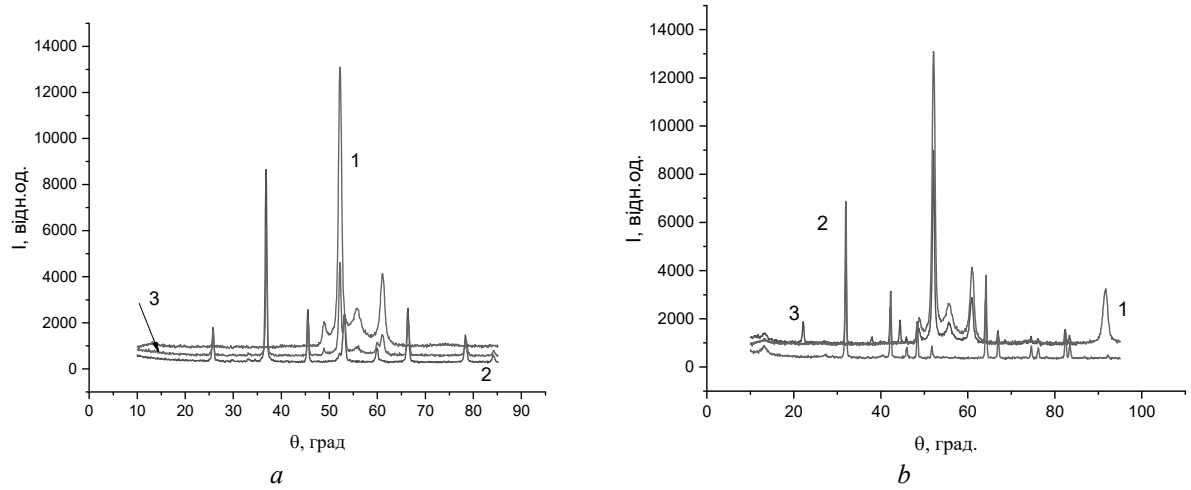

Fig. 1. Diffraction of NiCo (*1*), 0.13NiCo/0.87$BaTiO_3$ (*2*), and 0.7NiCo/0.3$BaTiO_3$ (*3*) composites – *a*; and NiCo (*1*), 0.13NiCo/0.87TiO_2 (*2*), and 0,7NiCo/0.3TiO_2 (*3*) – *b*

The values of ε′, ε″ at a frequency of 9 GHz for the NiCo/$BaTiO_3$ system are twice as high compared to NiCo/TiO_2 for the corresponding values of the NiCo content, which is due to the higher values of ε′, ε″ of the initial barium titanate. The dependence has a nonlinear dependence on the NiCo content (Fig. 2, curves *1*, *3*) and changes the slope at a content of 0.5 NiCo nanoparticles for both systems. When the NiCo content increases to 0.7, the values of ε′ increase one and a half times compared to the content of 0.5, and twice compared to the content of 0.13.

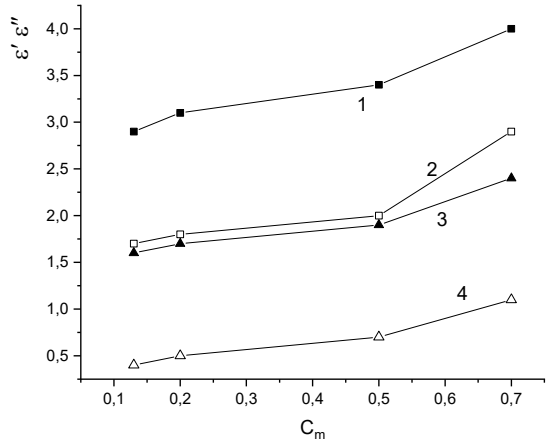

Fig. 2. ε′ (*1*, *3*) and ε″ (*2*, *4*) for the NiCo/$BaTiO_3$ (*1*, *2*) and NiCo/TiO_2 (*3*, *4*) composites at a frequency of 9 GHz on the NiCo content

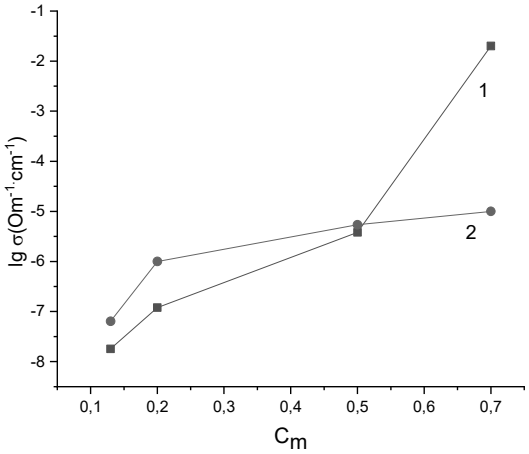

Fig. 3. Logarithm of electrical conductivity for the NiCo/$BaTiO_3$ (*1*) and NiCo/TiO_2 (*2*) composites on the NiCo content

The electrical conductivity in the NiCo/TiO_2 system (Fig. 3) varies within three orders of magnitude, which indicates the formation of a continuous percolation cluster of metal nanoparticles on the surface of TiO_2 dielectric particles. Note that a sharp change in the slope of the logarithmic conductivity curve occurs at a NiCo content of 0.16, which at first glance contradicts the experimental data of dielectric constant presented in Fig. 2. This is explained by the fact that the research was carried out by two different methods under different conditions

(different density of samples). When measuring electrical conductivity, the experimental sample is compacted 1.3 times, slightly increasing the density of the sample. The particles are at smaller distances, the number of contacts between the particles increases, which contributes to the increase in electrical conductivity. Dielectric measurements at 9 GHz are performed at bulk density because such data can be used to predict the dielectric properties of polymer composites with maximum filler content.

The additive content of NiCo nanoparticles was supposed to provide a higher level of electrical conductivity of the samples, however, it was noticed that during the synthesis of composites of the $0.7NiCo/0.3TiO_2$ system, chemical utensils are partially metallized, so not all synthesized particles settle on the proposed substrate and the real NiCo content is somewhat lower. In order to obtain information about the state of the surface of the substrate particles, an experimental determination of the value of the specific surface of the original TiO_2 powder was carried out by the method of thermal argon desorption. The obtained value of 10.9 cm^2/g is not high, therefore, obviously, the surface of these particles is not highly developed. The specific surface area of $BaTiO_3$ is 4.9 cm^2/g, which is half the corresponding value for TiO_2, obviously, the qualitative composition of the surface of barium titanate (surface charges) is fundamentally different from that of titanium dioxide.

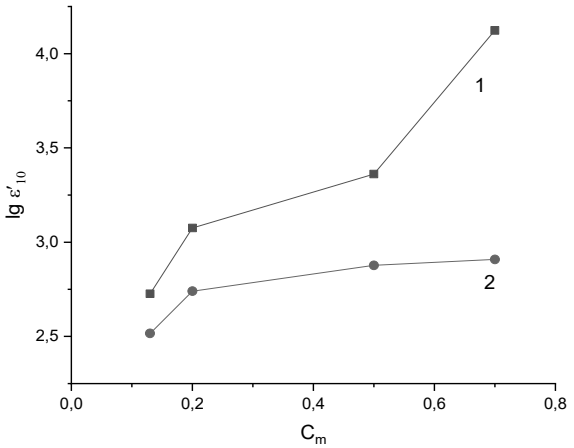

Fig. 4. ε'_{10} at a frequency of 10 kHz for the $NiCo/BaTiO_3$ (*1*) and $NiCo/TiO_2$ (*2*) composites on the NiCo content

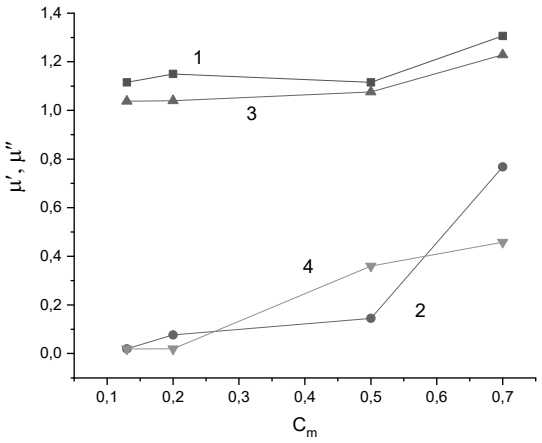

Fig. 5. μ′ (*1*, *3*) and μ″(*2*, *4*) at a frequency of 8 GHz for $NiCo/BaTiO_3$ (*1*, *2*) and $NiCo/TiO_2$ (*3*, *4*) composites on the NiCo content

At the first stage, a cluster of NiCo particles is formed on the surface of $BaTiO_3$ dielectric particles, at the second stage, clusters of conductive NiCo particles are formed upon contact with metal particles.

All obtained samples have pronounced magnetic properties. The study of the magnetic permeability at a frequency of 8 GHz of both systems was carried out at bulk density (Fig. 5). Magnetic losses increase with an increase in the content of metal nanoparticles and reach the highest values (tangent of the angle of magnetic losses = 0.59) for the $NiCo/BaTiO_3$ 0.7 composite. The presence of magnetic permeability and magnetic losses at microwaves is due to the natural ferromagnetic resonance in metal nanoparticles.

The thermal stability of the obtained composites was evaluated by the method of thermogravimetry (Fig. 6 *a*, *b*).

It can be seen from the figures that all composites are characterized by an increase in mass with increasing temperature, namely in the temperature range of 593, 733, 843, 893 K, which probably occurs due to the oxidation processes of metal particles, as was shown in [26]. It was found that composites with a content of 0.33 metal particles have a characteristic peak at 843 K, and composites with a content of 0.57 do not have it, however, all composites oxidize in the region of 733 K, only those with a lower content of metal particles oxidize less intensively, with at a lower speed.

A three-layer scheme was used to estimate the absorption coefficient of composites and their reflection [27]. In the model, different media are represented by corresponding wave resistances Z0i and wave numbers $k_i = 2\pi/\lambda_i$ n (i = 1, 2, 3): n – complex refractive index

$$Z_{03}' = Z_{02}\frac{Z_{03}+iZ_{02}tgk_2d}{Z_{02}+iZ_{03}tgk_2d}. \quad (1)$$

The reflection coefficient in the first medium

$$R = \frac{Z_{03}'-Z_{01}}{Z_{03}+Z_{01}} = \frac{Z_{02}(Z_{03}-Z_{01})+i(Z_{03}^2-Z_{01}Z_{03})tgk_2d}{Z_{02}(Z_{03}+Z_{01})+i(Z_{03}^2 0 Z_{01}Z_{03})tgk_2d}. \quad (2)$$

Absorption coefficient:

$$A = 1 - R - T\ . \quad (3)$$

The program for calculating frequency dependences of reflection and absorption coefficients in a complex form has been developed. The initial parameters are ε′, ε″, μ′, μ″ and sample thickness d.

Fig. 7 shows the dependences of the reflection coefficient for systems with $NiCo/BaTiO_3$ (*a*) and $NiCo/TiO_2$ (*b*) on the EMF frequency, calculated according to equations (1–3). Experimentally obtained values are shown by crosses. It can be seen from the graphs that the experimental indicators differ from the theoretical ones within the experimental error. At small values of ε′, the value of the reflection coefficient is low, with an increase in the values of ε′, which occurs when the NiCo content increases, the reflection coefficient increases and significant EMF energy is reflected, not absorbed. The absorption coefficient (Fig. 8) characterizes the amount of energy that remained in the material of a given thickness during the passage of EMW. Composites with the composition $BaTiO_3$ have large values of ε′, which strongly affects absorption due to reflection.

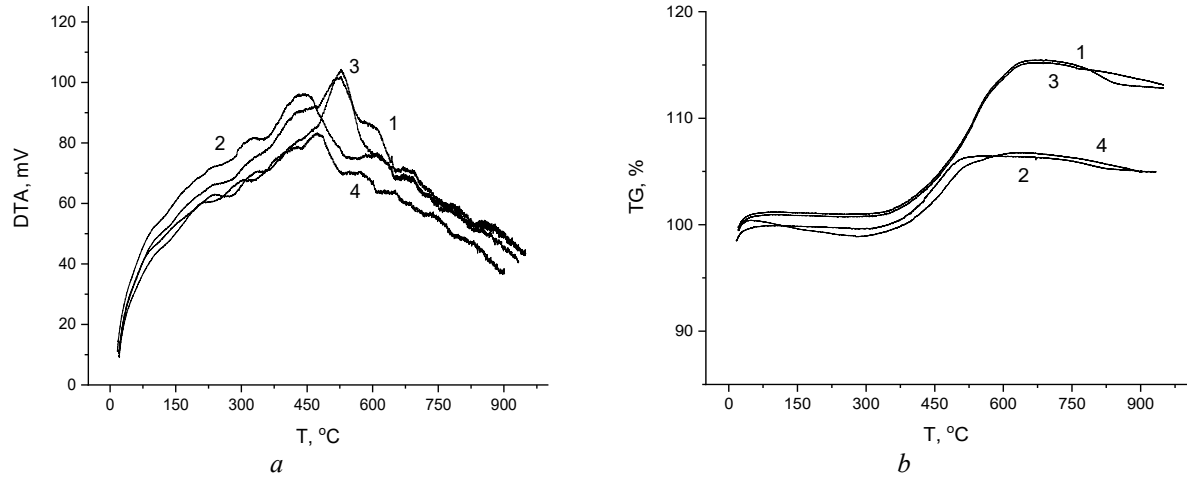

a *b*

Fig. 6. DTA (*a*) and TG (*b*) of composites: $0.33NiCo/0.67BaTiO_3$ (*1*); $0.57NiCo/0.43BaTiO_3$ (*2*); $0.33NiCo/0.67TiO_2$ (*3*); $0.57\ NiCo/0.43TiO_2$ (*4*)

The minima on the frequency dependence of the reflection coefficient are caused by the phenomenon of interference when waves are reflected from two faces of the sample and depends on its thickness $d = \frac{\lambda}{4\sqrt{\varepsilon\prime}}$, as well as on ε′. When the value of the real term of the complex permittivity, which is observed when the content of metal particles in the composite changes, changes, the position of the minimum frequency changes.

In the frequency range of 20–35 GHz, the reflectance values for composites with titanium dioxide decrease more strongly, which is a manifestation of the next minimum. Under these conditions, the reflection extremum is observed at the optical thickness of the layer $\lambda_0/4$, the next minimum at $\lambda_0/2$, which corresponds to the phase thickness of the layer π. Therefore, extrema are observed at $\frac{\lambda_0}{4}k$, where k is a natural number.

Fig. 7 *b* shows that the absorption level for the $0.7NiCo/0.3BaTiO_3$ composite significantly decreases with frequency compared to other composites. Obviously, a significant degree of metallization of the original ferroelectric causes a high level of EMW reflection from the metal phase, as a result of which the level of absorption decreases.

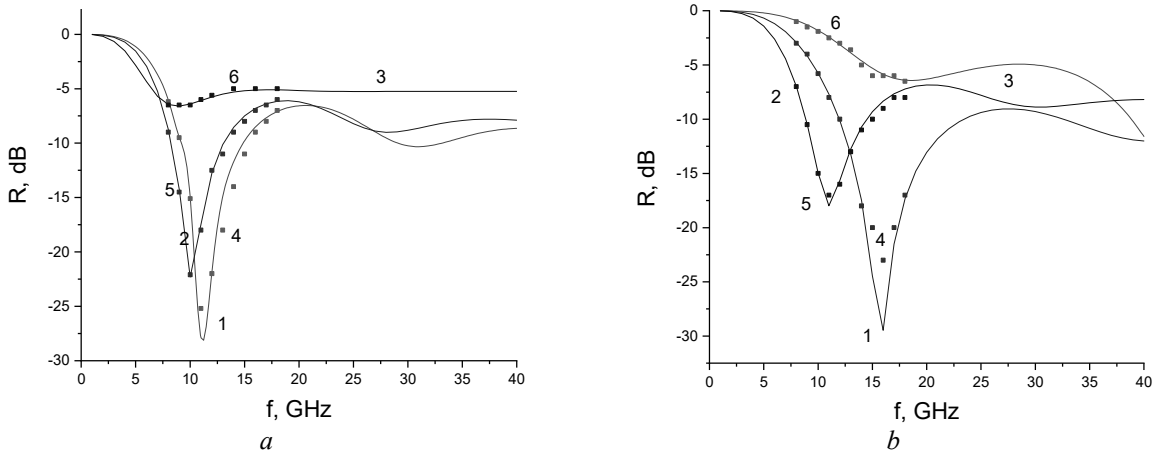

Fig. 7. The reflection coefficient for systems with $NiCo/BaTiO_3$ (*a*) and $NiCo/TiO_2$ (*b*) on the EMW frequency at given experimentally determined values of ε′, ε″, μ′, μ″ shown in Figs. 2, 5 at a thickness of 4 mm, the content of NiCo nanoparticles: *1*, *4* – 0.13; *2*, *5* – 0.5; *3*, *6* – 0.7. Lines (*1*, *2*, *3*) show theoretical curves, experimental points are represented by squares (*4*, *5*, *6*)

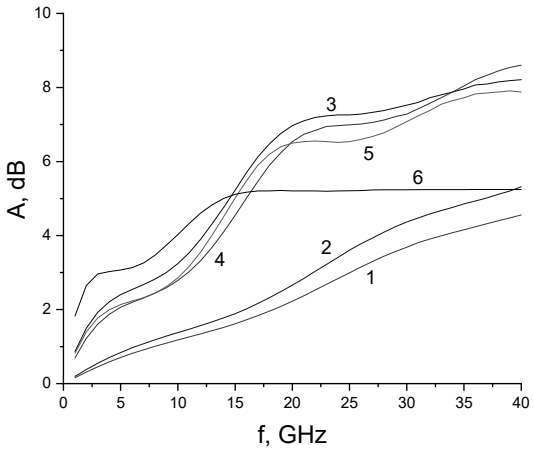

Fig. 8. The absorption coefficient A on the EMW frequency at given experimentally determined values of ε′, ε″, μ′, μ″ shown in Figs. 2, 5 at the thickness of 4 mm for composites: $0.13NiCo/0.87TiO_2$ (*1*); $0.2NiCo/0.8TiO_2$ (*2*); $0.7NiCo/0.3TiO_2$ (*3*); $0.13NiCo/0.87BaTiO_3$ (*4*); $0.2NiCo/0.8BaTiO_3$ (*5*); $0.7NiCo/0.3BaTiO_3$ (*6*)

CONCLUSIONS

The methods of $NiCo/BaTiO_3$ and $NiCo/TiO_2$ nanostructured systems synthesis were developed, and composites were obtained by the method of chemical precipitation from a solution with different content of metal nanoparticles.

X-ray phase analysis proved the presence of Ni and Co phases and the absence of initial carbonates. The values of the real and imaginary components of the complex permittivity for the $NiCo/BaTiO_3$ composites are higher in comparison with $NiCo/TiO_2$ by an average of 1.5 times at a frequency of 9 GHz. The electrical conductivity at low frequencies for $NiCo/BaTiO_3$ is higher only with a content of 0.7 NiCo by 4 orders of magnitude; composites with a lower content of metal particles have lower values for $NiCo/BaTiO_3$, which is due to the specific surface

area of the components ($\sigma(TiO_2)$ = 10.9 cm^2/g, $\sigma(BaTiO_3)$ = 4.9 cm^2/g).

It was found that the composites provide high dielectric properties at microwaves with a low content (up to 0.2 volume fraction) of NiCo nanoparticles, as well as significant magnetic losses due to natural ferromagnetic resonance.

Theoretical approaches were used to estimate reflection coefficients, EMF absorption for composites from the radiation frequency and the position of the minima of these characteristics, which agree satisfactorily with the experiment. The obtained composites can be promising components for obtaining composite systems and paints for protection against electromagnetic radiation.

Синтез та електрофізичні властивості наноструктурних композитів $NiCo/BaTiO_3$ та $NiCo/TiO_2$

С.М. Махно, О.М. Лісова, Г.М. Гуня, П.П. Горбик, М.Т. Картель

Університет технологій, Ніньбо
Фенгуа роад, 201, Ніньбо, 315211, Китай
Китайсько-український інститут промислових технологій нових матеріалів
буд. Кечуанг, 777, Жонгуан роад, Ніньбо, 315211, Китай
Інститут хімії поверхні ім. О.О. Чуйка Національної академії наук України
вул. Генерала Наумова, 17, Київ, 03164, Україна, oksana.garkusha@gmail.com

Нанокомпозити, що містять компоненти з напівпровідниковими, сегнетоелектричними та феромагнітними властивостями, привертають значну увагу фахівців завдяки широкому спектру можливих застосувань: каталіз та електрокаталіз, електродні матеріали для сонячних і паливних елементів, конденсатори, електричні та біосенсори, антикорозійні покриття та багато іншого. В останні роки як фундаментальний, так і прикладний інтерес до цього напряму досліджень зумовлений можливістю створення нового типу керованих НВЧ-пристроїв і засобів.

Метою роботи є розробка методів синтезу наноструктурованих NiCo композитів на основі $BaTiO_3$ і TiO_2, а також встановлення відмінностей і закономірностей їхніх фізико-хімічних властивостей. Отримано дві серії зразків з різним вмістом наночастинок NiCo на основі оксиду титану (TiO_2) і титанату барію ($BaTiO_3$). Частинки NiCo отримано методом хімічного осадження карбонатів нікелю та кобальту в рівних частинах з розчину гідразингідрату при 350 K.

Результати рентгенофазового аналізу свідчать про хімічну чистоту одержаних зразків. Значення ε′, ε″ на частоті 9 ГГц для системи $NiCo/BaTiO_3$ вдвічі вищі порівняно з $NiCo/TiO_2$ для відповідних значень вмісту NiCo, що зумовлено вищими значеннями ε′, ε″ вихідного титанату барію. Електропровідність системи $NiCo/BaTiO_3$ змінюється на шість порядків, що свідчить про утворення суцільного перколяційного кластера металевих частинок на поверхні діелектричних частинок $BaTiO_3$. Композити термостійкі до 630 K, що підтверджено методом термогравіметрії та мають виражені магнітні властивості.

Розроблено програму для розрахунку частотних залежностей коефіцієнтів відбиття та поглинання в комплексному вигляді. Розраховано коефіцієнти поглинання електромагнітних хвиль для композитів від частоти випромінювання та положення мінімумів цих характеристик, які задовільно узгоджуються з експериментом. Отримані композити можуть бути перспективними компонентами для отримання композитних систем і фарб для захисту від електромагнітного випромінювання.

***Ключові слова**: нанокомпозити, наночастинки, феромагнетик, електромагнітні хвилі, електропровідність*

REFERENCES

1. Arshad M., Khan W., Abushad M., Nadeem M., Husain S., Ansari A., Chakradhary K.V. Correlation between structure, dielectric and multiferroic properties of lead free Ni modified $BaTiO_3$ solid solution. *Ceram. Int.* 2020. **46**(17): 27336.
2. Nematollahi R., Ghotbi C., Khorasheh F., Larimi A. Ni-Bi co-doped TiO_2 as highly visible light response nano-photocatalyst for CO_2 photo-reduction in a batch photo-reactor. *J. CO_2 Util.* 2020. **41**: 101289.
3. Ray S.K., Cho J., Hur J. A critical review on strategies for improving efficiency of $BaTiO_3$-based photocatalysts for wastewater treatment. *J. Environ. Manage*. 2021. **290**: 112679.
4. Sharma M., Gaur A. Fabrication of PVDF/$BaTiO_3$/NiO nanocomposite film as a separator for supercapacitors. *J. Energy Storage*. 2021. **38**: 102500.
5. Abbas T., Tahir M. Tri-metallic Ni–Co modified reducible TiO_2 nanocomposite for boosting H_2 production through steam reforming of phenol. *Int. J. Hydrogen Energy*. 2021. **46**(13): 8932.
6. Xie S., Li L., Jin L., Wu Y., Liu H., Qin Q., Wei X., Liu J., Dong L., Li B. Low temperature high activity of M (M = Ce, Fe, Co, Ni) doped M-Mn/TiO_2 catalysts for NH_3-SCR and in situ DRIFTS for investigating the reaction mechanism. *Appl. Surf. Sci*. 2020. **515**: 146014.
7. Malathi S., Pakrudheen I., Kalkura S.N., Webster T.J., Balasubramanian S. Disposable biosensors based on metal nanoparticles. *Sens. Int.* 2022. **3**: 100169.
8. Alwarappan S., Nesakumar N., Sun D., Hu T.Y., Li C.-Z. 2D metal carbides and nitrides (MXenes) for sensors and biosensors. *Biosens. Bioelectron*. 2022. **205**: 113943.
9. Aroua W., Derbali J., Raaif M., Malek F.A. Design of a new label free active biosensor based on metallic nanoparticles-doped graphene nanodisk platform. *Opt. Commun*. 2022. **515**: 128220.
10. Zhang G., Fürst M., Lengauer W., Zhang J., Ke Z., Xu X., Wu H. On the use of TiO_2 in Ti(C,N)-WC/Mo_2C-(Ta,Nb)C-Co/Ni cermets. International. *Int. J. Refract. Met. Hard Mater. International*. 2020. **91**: 105274.
11. Kumar A., Kashyap M.K., Kumar S., Kumar P., Asokan K. Effect of dilute co-doping of Ni and Cr on physical properties of TiO_2 nanoparticles. *Vacuum*. 2020. **181**: 109658.
12. Yousefi E., Sharafi S., Irannejad A. The structural, magnetic, and tribological properties of nanocrystalline Fe-Ni permalloy and Fe-Ni-TiO_2 composite coatings produced by pulse electro co-deposition. *J. Alloys Compd*. 2018. **753**: 308.
13. Gupta P., Mahapatra P.K., Choudhary R.N.P. Investigation on structural and electrical properties of Co and W modified $BaTiO_3$. *Ceram. Int., Part B.* 2019. **45**(17): 22862.
14. Hasan M., Akther Hossain A.K.M. Structural, electronic and optical properties of strontium and nickel co-doped $BaTiO_3$: A DFT based study. *Comput. Condens. Matter*. 2021. **28**: 1.
15. Liu Q., Cao Q., Bi H., Liang C., Yuan K., She W., Yang Y., Che R. CoNi@SiO_2 @TiO_2 and CoNi@air@TiO_2 microspheres with strong wideband microwave absorption. *Adv. Mater*. 2016. **28**(3): 486.
16. Zhao J., Lu Y.J., Ye W.L., Wang L., Liu B., Lv S.S., Chen L.X., Gu J.W. Enhanced wave- absorbing performances of silicone rubber composites by incorporating C-SnO_2-MWCNT absorbent with ternary heterostructure. *Ceram. Int*. 2019. **45**(16): 20282.
17. Yuan X.Y., Wang R.Q., Huang W.R., Liu Y., Zhang L.F., Kong L., Guo S.W. Lamellar vanadium nitride nanowires encapsulated in graphene for electromagnetic wave absorption. *Chem. Eng. J.* 2019. **378**: 122203.
18. Yang X.T., Fan S.G., Li Y., Guo Y.Q., Li Y.G., Ruan K.P., Zhang S.M., Zhang J.L., Kong J., Gu J.W. Synchronously improved electromagnetic interference shielding and thermal conductivity for epoxy nanocomposites by constructing 3D copper nanowires/thermally annealed graphene aerogel framework. *Composites, Part A*. 2020. **128**: 105670.
19. Xiong J., Xiang Z., Deng B., Wu M., Yu L., Liu Z., Cui E., Pan F., Liu R., Lu W. Engineering compositions and hierarchical yolk-shell structures of NiCo/GC/NPC nanocomposites with excellent electromagnetic wave absorption properties. *Appl. Surf. Sci.* 2020. **513**: 145778.
20. Deng B., Xiang Z., Xiong J., Liu Z., Yu L., Lu W. Sandwich-like Fe&TiO_2@C nanocomposites derived from MXene/Fe-MOFs hybrids for electromagnetic absorption. *Nano Micro Lett*. 2020. **12**: 55.
21. Li X., Wang Z., Xiang Z., Zhu X., Dong Y., Huang C., Cai L., Lu W. Biconical prisms Ni@C composites derived from metal-organic frameworks with an enhanced electromagnetic wave absorption. *Carbon*. 2021. **184**: 115.
22. Seiti D., Viana F., Jesus A., De Oliveira A., Charles K.R., Jimenez P., Milton F.P., Eiras J.A., Santos G.M., Garcia D. Synthesis and multiferroic properties of particulate composites resulting from combined size effects of the magnetic and ferroelectric phases. *Ceram. Int.* 2022. **48**(1): 931.
23. An F., Zi M., Chen Q., Liu C., Qu K., Jia T., Huang M., Zhong G. Flexible room-temperature multiferroic thin film with multifield tunable coupling properties. *Mater. Today Phys.* 2022. **23**: 100615.

24. Kossar S., Amiruddin R., Rasool A., Santhosh Kumar M.C., Katragadda N., Mandal P., Ahmed N. Study on ferroelectric polarization induced resistive switching characteristics of neodymium-doped bismuth ferrite thin films for random access memory applications. *Curr. Appl. Phys*. 2022. **39**: 221.
25. Ganyuk L.M., Ignatkov V.D., Makhno S.M., Soroka P.M. Investigation Researching the electrical power of fibrous material. *Ukr. J. Phys.* 1995. **40**(6): 627.
26. Bogatyrov V.M., Borisenko M.V., Oranska O.I., Galaburda M.V., Makhno S.M., Gorbyk P.P. Synthesis and properties of Ni/C, Co/C, and Cu/C metal-carbon nanocomposites with high metal content. *Surface*. 2017. **24(9)**: 136.
27. Moskaluk V.O., Saurova T.A. *Field theory*. (Kyiv: Sikorsky KPU, 2018).

Received 07.11.2022, accepted 05.06.2023